scientific reports

Check for updates

OPEN

MPPT algorithm based on metaheuristic techniques (PSO & GA) dedicated to improve wind energy water pumping system performance

Abdelhak Bouchakour[1], Laid Zarour[2], Noureddine Bessous[3], Mohcene Bechouat[4], Abdelhalim Borni[1], Layachi Zaghba[1], Abdelaziz Rabehi[5], Abdullah Alwabli[6], Mohammed El-Abd[7]✉ & Sherif S. M. Ghoneim[8]

This paper presents a comparative study between four techniques recently used to improve the wind energy conversion system (WECS) to water pumping systems. The WECS is a renewable energy source which has developed rapidly in recent years. The use of the WECS in the water pumping field is a free solution (economically) compared to the use of the electricity grid supply. The control of WECS, equipped with a permanent magnet synchronous generator, has the objective of carefully maximising power generation. A comparative study between the proposed Fuzzy Logic Control, optimised using a genetic algorithm and particle swarm optimisation algorithm, and the conventional Perturb and Observe MPPT method using Matlab/Simulink, is presented. The performance of the proposed system has been verified against the generated output voltage, current and power waveforms, intermediate circuit voltage waveform, and generator speed. The presented results demonstrate the effectiveness of the control strategy applied in this work.

Keywords MPPT, Wind energy, P&O, Fuzzy logic control, PSO, GA

List of symbols

P_w	Power turbine (W)
C_p	Power coefficient
V_w	Speed wind (m/s)
ρ	Air mass
R	Blades of length (m)
λ	The speed point ratio
β	The blade step angle
$\Delta\Omega_{ref}$	Variation of the turbine reference speed (m/s)
ΔP_{ref}	Variation of the turbine reference power (W)
V_{dq}	Direct & quadrature voltage (V)
i_{dq}	Direct & quadrature current (A)
ω_m	Mechanical speed (rad/s)
T_e	Electromagnetic torque (Nm)

[1]Unité de Recherche Appliquée en Energies Renouvelables, URAER, Centre de Développement des Energies Renouvelables, CDER, 47133 Ghardaïa, Algeria. [2]Electrotechnical Laboratory Faculty of Technical Sciences, University of Constantine 1, Constantine, Algeria. [3]Department of Electrical Engineering, Faculty Technology, University of El Oued, 39000 El-Oued, Algeria. [4]Department of Automatics and Electro Mechanics, Faculty of Science and Technology, University of Ghardaïa, 47000 Ghardaïa, Algeria. [5]Telecommunications and Smart Systems Laboratory, University of ZianeAchour, 17000 Djelfa, Algeria. [6]Department of Electrical Engineering, College of Engineering and Computing in Al-Qunfudhah, Umm Al-Qura University, Mecca, Saudi Arabia. [7]College of Engineering and Applied Sciences, American University of Kuwait, Salmiya, Kuwait. [8]Department of Electrical Engineering, College of Engineering, Taif University, 21944 Taif, Saudi Arabia. ✉email: melabd@auk.edu.kw

T_L	Load torque (Nm)
L_{dq}	Direct & quadrature inductor (H)
Rs	Series resistance (Ohm)
V_{bus}	DC-link voltage (V)
Φ_e	PMSM flux in Web
P_1,….P_{21}	Membership function
J_k	Objective function
X^{best}	Best position obtained
kp2, ki2 kp1,ki1	The PI regulator gains
P_1, P_2, P_3, K_1, K_2, K_3	The normalisation factors
X*	The optimal solution
c0, c1 and c2	The inertia factor
$f_{1,2,3}$	The switching functions of the inverter
V_{fa}, V_{fb}, V_{fc}	The output voltages of the inverter
I_{opt}	Optimum current
V_{opt}	Optimum Voltage

Wind energy, the most recently developed green energy source, is being transformed from a small to a major power source in the field of energy systems, due to power electronics. Solar, wind, and hydraulics are the most popular sources[1].

Wind energy is a renewable energy that requires no fuel, creates no greenhouse gases, and produces no toxic or radioactive waste. Wind energy produces electricity without degrading the quality of the air, without polluting the waters, and without polluting the soil. Wind power guarantees security of supply, in the face of fluctuating oil prices, with the possibility of reducing electricity bills. It also plays an important role in preserving biodiversity by combating climate change. The technology continues to improve, with wind turbines now being more powerful, and their efficiency has increased tenfold in the last ten years. Thus, a 12 MW wind farm, made up of four to six wind turbines, can cover the electricity consumption needs of nearly 12,000 people and avoids the emission of 8000 tons of CO_2[1,2.]

As a photovoltaic system (PVS) occupies a large area for limited maximum power, wind energy also has the peculiarity of having a higher yield in winter (wind is generally stronger in the cold season). This is an important advantage because of the high costs usually ocurring during the winter period[3,4]. Agricultural watering requirements are often at their highest during sunny hours when a wind energy system can pump more water[5,6].

The development of a dependable and efficient wind energy conversion system (WECS) to address the problem of water scarcity in desert locations is a very interesting project. However, WECS have nonlinear characteristics and only have one maximum power point (MPP). The operating point, as well as the MPP, will fluctuate as the meteorological conditions change. As a result, an online control approach, called maximum power point tracking (MPPT), must be utilised to track the WECS' maximum output power under various operating situations.

MPPT commands can be classified according to the type of implementation, the input parameters and the type of search they perform. However, it is more interesting to classify them according to criteria such as precision, speed and convergence towards the maximum power point. The MPPT control must have a significant level of simplicity favouring low consumption and a reasonable cost. In addition, regarding its performance, the MPPT command must have a good dynamic and static behavior to ensure rapid and precise adaptation to climate change. Several methods exist in the literature, classic method such as P&O, incremental conductance and intelligent methods such as: fuzzy logic, PSO and GA.

Because of their compact size, self-excitation, high reliability, cheap maintenance, lack of a gearbox system, and low noise, permanent magnet synchronous generators (PMSGs) were employed in this study[6,7].

The WECS was optimised using a perturb and observe (P&O) approach. The difference in output power between the current and prior states is used to define the system control in this approach. Furthermore, the P&O algorithm's mechanism has a set step size, which restricts its efficacy. As a result, a number of academics have developed a variety of variable step MPPT algorithms to address this issue[8,9]. The objective of the control strategies, based on the conventional proportional-integral controllers (PICs), is to ensure the robustness and the stability of the WECS.

The best conventional proportional-integral controllers depend on the parameter calculations of nonlinear systems (electrical systems)[10,11]. However, the difficulty is characterised by its high sensitivity to the variable parameters.

In order to manage the features of nonlinear dynamic systems, this study explores the performance of fuzzy logic control (FLC), which takes a different approach than proportional-integral PI methods.

Generally speaking, the FLC depends on the designer's fine-tuning membership functions (MF), while many of the classical FLCs are based on a fixed membership function (MF) and a static rule base. However, they are not sufficient to solve nonlinear systems with a high degree of uncertainty[12,13].

So, adaptive filtering techniques have been used, based on the Continuous Mixed-Normal (CMPN) algorithm. This allows the FLC scale factors to be updated online and improves the performance of a wind generator under variable speed connected to a water pump[8,14].

The benefits of a permanent magnet synchronous machine (PMSM) attached to a water pump device have piqued the attention of researchers and industry for use in a variety of applications. It generates the air gap magnetic field of permanent magnets rather than electromagnets[4]. Quick dynamics, efficient operation, and strong compatibility with various applications are all advantages of PMSM with high-level energy permanent magnet materials, but only if they are properly managed. The controller is used to solve the PMSM's nonlinearity

problem and to obtain quicker response times[5]. The advancement of power electronics and electric technologies has enhanced the use of PMSM for a wide range of applications in many control systems.

Motivated by the above discussion, the work presented in this paper concerns a comparative study of MPPT algorithms based on P&O, FL controller and their optimisations, using GA and PSO methods for WECS connected to a moto-pump. These methods are compared through Matlab/Simulink software to show the performances of each MPPT technique under different weather conditions, for transient, dynamic and steady state responses.

Overview of the wind energy water pumping system

A wind pump is a complex system that consists of different interacting elements, one of which acts on the other in different ways and within limits imposed by the control strategies employed. The modelling of the different elements of the system, such as the wind turbine, the inverter, the motor, the pump and the hydraulic circuit, involves knowledge of several disciplines: meteorology, electronics and electrical engineering, and hydraulics, and requires a good understanding of the interactions between them.

The studied wind energy conversion system consists of two parts. The power side system is a wind turbine with a three phase permanent magnet synchronous moto-pump, through a rectifier, a boost converter and a three level AC inverter. The system is controlled via the MPPT strategy based on the fuzzy logic controller and optimised by the GA and PSO. The overall structure of the system is shown in Fig. 1@@[15].

Turbine modelling

The power value is a function of the air mass and the velocity V_w[14,16].

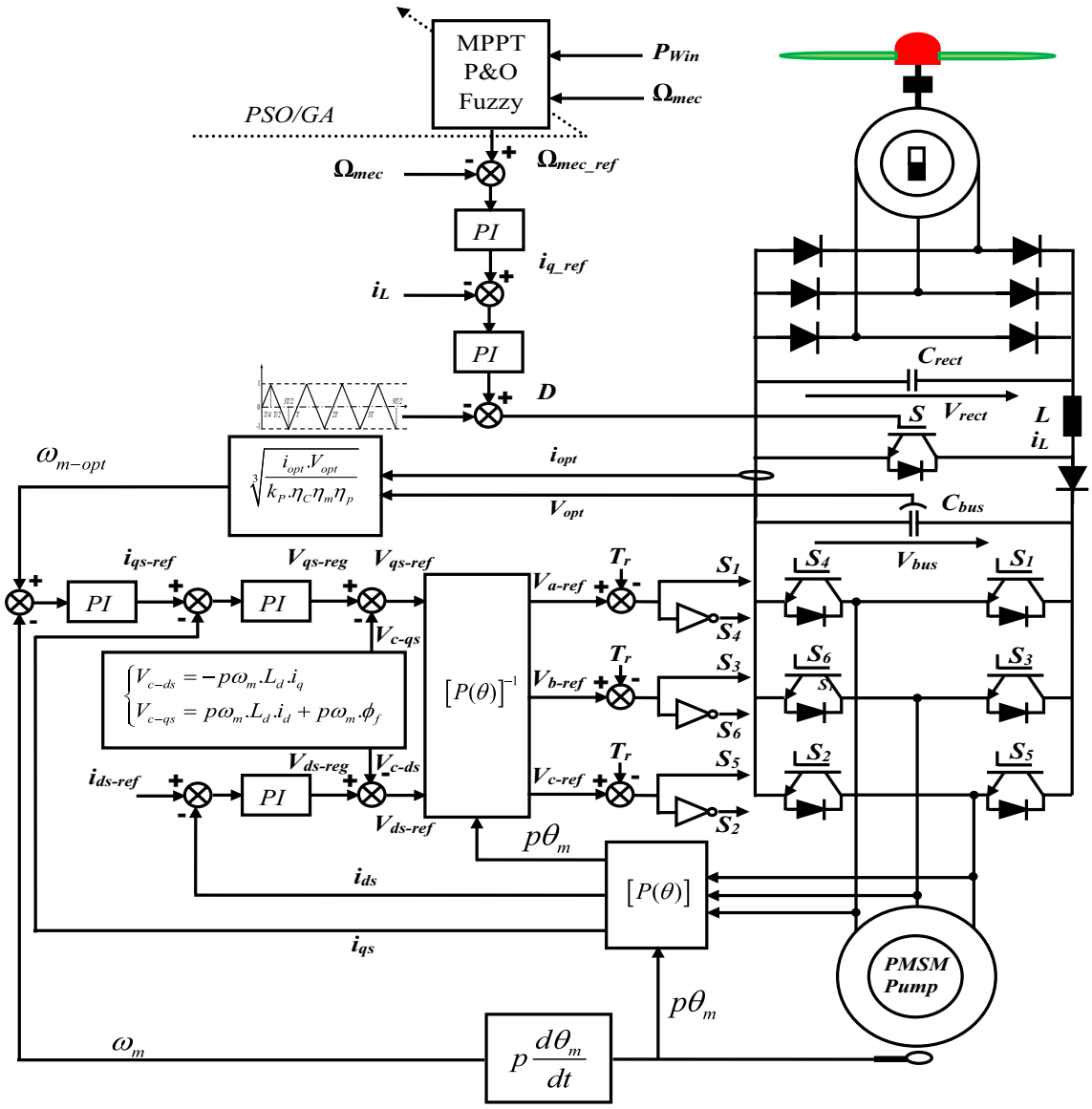

Figure 1. Overall diagram of the Wind Energy Water Pumping System.

$$P_w = \frac{1}{2}\rho.\pi.R^2.C_p.(\lambda,\beta).V_w^3 \quad (1)$$

where R is the blade length, K is the gain multiplier, and C_p is the value which depends on the speed point ratio (λ) and the blade step angle (β), depending on the turbine characteristics (Fig. 2a).

$$C_p = 0,5.((\frac{98}{\lambda'}) - 0,4\beta - 5)\exp(\frac{-16,5}{\lambda'}) \quad (2)$$

and

$$\lambda' = 1/(\frac{1}{\lambda + 0,08\beta} - \frac{0,035}{\lambda^3 + 1})$$

Figure 2 shows $P_w = f(\Omega)$ under different wind speeds. Each curve shows an optimum power point, which corresponds to a certain rotation speed.

PMSM modelling

The permanent magnet synchronous machine (PMSM) has become attractive and competes with the asynchronous machines in the field of electric drive systems because of its advantage in the elimination of slip losses. For this type of machine, the inductor is replaced by permanent magnets, creating the excitation field. This also has the advantage of eliminating brushes and rotor losses, resulting in high efficiency, and requiring no maintenance throughout its life[17].

The differential model of the PMSM is given by[18]:

$$\begin{cases} \frac{di_d}{dt} = -\frac{R_S}{L_d} i_d + p\omega \frac{L_q}{L_d} i_q - \frac{V_d}{L_d} \\ \frac{di_q}{dt} = -p\omega \frac{L_d}{L_q} i_d - \frac{R_S}{L_q} i_d - \frac{V_q - p\omega \cdot \varphi_e}{L_q} \end{cases} \quad (3)$$

The electromagnetic torque will be expressed by:

$$T_e = p \cdot \left((L_d - L_q) \cdot i_{sd} + \varphi_f\right) \cdot i_{qs} \quad (4)$$

The mechanical equation is written:

$$\frac{d\omega_m}{dt} = \frac{p}{J} \cdot \left((L_d - L_q) i_{ds} + \phi_f\right) \cdot i_{qs} - \frac{f}{J} \cdot \omega_m - \frac{p}{J} \cdot T_L \quad (5)$$

PMSM control

The main advantage of MCC is that it is easily controlled, as the flow and torque are decoupled and are controlled independently. For an MSAP, decoupling no longer exists, which makes the machine difficult to control. This difficulty lies in the fact that there is a coupling between the input variables (voltage, frequency) and the output variables (torque, speed). To achieve a control similar to MCC, we apply the vector control[19,20].

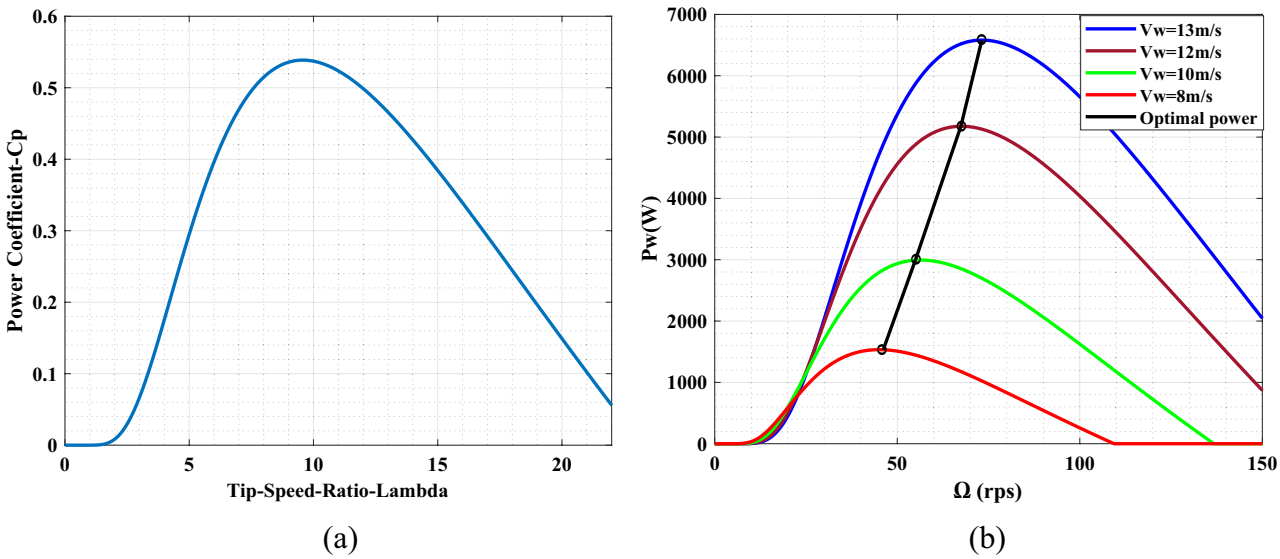

Figure 2. (**a**) Power and (**b**) power coefficient characteristics at different wind level.

To control the torque (Eq. (2)), it is necessary to control the direct and quadrature components of the current. For a synchronous machine with smooth poles ($L_d = L_q$), the torque will be:

$$T_e = p\varphi_f i_{qs} \tag{6}$$

As the flux of the magnets is constant, the electromagnetic torque obtained becomes proportional to the current I_q.

$$\begin{cases} V_d = R_s \cdot i_{ds} + L_d \dfrac{di_{ds}}{dt} - p\omega_m \cdot L_d \cdot i_{qs} \\ V_q = R_s \cdot i_{qs} + L_q \dfrac{di_{qs}}{dt} + p\omega_m \cdot L_q \cdot i_{ds} + p\omega_m \cdot \phi_f \end{cases} \tag{7}$$

Adjustment of the internal loop of the current I_{dqs}. The expression of the reference current i_{qs_ref} is given by:

$$i_{qs-ref} = \frac{T_{e-ref}}{\phi_f} \tag{8}$$

The current regulation loop i_{dqs} can be represented by the block diagram in Fig. 3.
The closed loop transfer function is as follows:

$$\frac{i\_dqs}{i\_dqs-reg} = \frac{(k\_pdqs \cdot s + k\_idqs)\frac{1}{L_{dq}}}{\left(s^2 + \frac{1}{L_{dq}}(R_s + k\_pdqs) \cdot s + \frac{k\_idqs}{L_{dq}}\right)} \tag{9}$$

The characteristics polynomial is:

$$P(s) = s^2 + \frac{1}{L_{dq}}(R_s + k_{pdqs}) \cdot s + \frac{k_{idqs}}{L_{dq}} \tag{10}$$

Through a simple comparison of Eq. (9) and (10), the gains k_{pdqs} and k_{idqs} are expressed by: $k_{pdqs} = 2L_{dq}\rho - R_s$ and $k_{idqs} = 2L_{dq}\rho^2$.

Adjustment of the external speed loop. The speed regulator is used to determine the reference torque in order to maintain the corresponding speed (Fig. 4). The mechanical equation gives:

$$\frac{\omega_m(s)}{T_e(s)} = \frac{p}{f + J \cdot s} \tag{11}$$

By associating a PI regulator with this function, it will be:
The parameters of PMSG are given in Table 1.
The closed loop transfer function, calculated from the previous diagram, is given by:
The characteristics polynomial is:

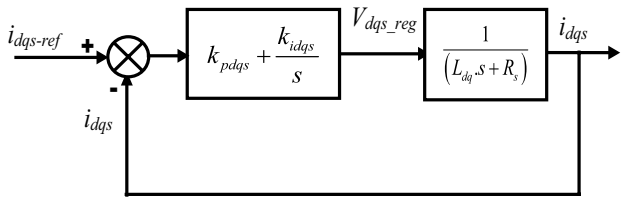

Figure 3. Current regulation block diagram i_{dqs}.

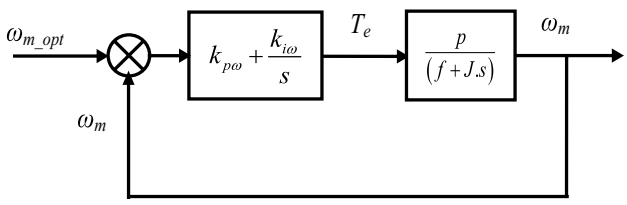

Figure 4. Speed control functional diagram.

Rated power	Rated Voltage	Frequency	Number of poles	Inertia constant
5.5 Kw	200 V	50 Hz	12	7.856 kg m^2
Stator Resistance	d-axis Reactance	q-axis Reactance	Field flux	Nominal speed
0.3676 Ω	0.00355 H	0.00355 H	0.2867 V. s	70 rps

Table 1. PMSG parameters.

$$P(s) = s^2 + \frac{f + k_{p\omega} \cdot p}{J} \cdot s + \frac{k_{i\omega} \cdot p}{J} = 0 \tag{13}$$

Comparing Eq. (12) and (13), the gains k_{pdqs} and k_{idqs} are expressed by:$k_{pdqs} = 2L_{dq}\rho - R_s$ and $k_{idqs} = 2L_{dq}\rho^2$

Static decoupling
The PMSM is supplied by the voltage inverter, according to Eq. (1), and the stator voltages are expressed by:

$$\begin{cases} V_{ds-ref} = V_{ds-reg} - V_{c-ds} \\ V_{qs-ref} = V_{qs-reg} - V_{c-qs} \end{cases} \tag{14}$$

Equation (14) shows that V_d and V_q depend on the stator currents on the axes (dq), which leads us to implement a decoupling. This coupling is eliminated by a compensation method. The latter consists of regulating the currents while neglecting the coupling terms, which will be added to the outputs of the current regulators in order to obtain reference voltages to supply the inverter. So:

$$\begin{cases} V_{c-ds} = -p\omega_m.L_d.i_q \\ V_{c-qs} = +p\omega_m.L_d.i_d + p\omega_m.\phi_f \end{cases} \tag{15}$$

The reference speed is based on the optimum power of the wind generator. It is given by the following relation:

$$\omega_{opt} = \sqrt[3]{\frac{I_{opt}.V_{opt}}{k_p.\eta_p.\eta_m.\eta_c.\eta_h}} \tag{16}$$

Modelling of the DC/AC static converter

A DC/AC inverter is included between the wind turbine and the motor pump to convert the direct voltage from the wind turbine into three-phase alternating voltage with a variable frequency, in order to feed the PMSM.

The output voltages of the inverter are given by[21]:

$$\begin{bmatrix} V_{fa} \\ V_{fb} \\ V_{fc} \end{bmatrix} = \frac{1}{3} V_{bus} \begin{bmatrix} 2 & -1 & -1 \\ -1 & 2 & -1 \\ -1 & -1 & 2 \end{bmatrix} \begin{bmatrix} f_1 \\ f_2 \\ f_3 \end{bmatrix} \tag{17}$$

$f_{1,3,5}$ are the switching functions of the inverter transistors.

Pump Modelling

The centrifugal pump is mainly characterised by a load torque proportional to the square of the motor speed, which is of the following form[22]:

$$T_L = k\omega_m^2 \tag{18}$$

where $k = \frac{P_L}{\omega_m^3}$.

MPPT control

The tracking method, known as maximum power point tracking (MPPT), is a command allowing the operation of a nonlinear electrical generator to permanently produce its maximum power[23,24].

Conventional tuning methods are based on adequate modelling of the system to be tuned and analytical processing using the transfer function or state equations. Unfortunately, these are not always available.

A wind energy water pumping system is difficult to control automatically. This difficulty comes from: their nonlinearity, the variation of their parameters, and the quality of the measurable variables. These difficulties led us to the development of new optimisation techniques.

The novelty presented in this article concerns the combination of classical optimisation methods (P&O) and metaheuristic optimisation techniques (PSO, GA). The MPPT approach relies on search algorithms (P&O, FL, FL-PSO, and FL-GA) to approximate the power limit curve without disrupting the system's normal operation.

P&O technique

The perturbation and observation (P&O) technique is widely used in industrial applications. As the algorithm is simple to implement, the objective process is to interrupt the system by increasing or decreasing the module's operating speed and observing its influence on the line's output power[5,9,25].

MPPT using FLC technique

Fuzzy logic is a very powerful problem solving technique with wide applicability in control and decision making. Fuzzy logic is very useful when the mathematical model of a problem does not exist or exists but is difficult to implement or is too complex to be evaluated quickly enough for real-time operations. Fuzzy logic is also assumed for situations where there are large uncertainties and unknown variations in system parameters and structures, such as wind power[13,26].

However, there is no general procedure for designing a fuzzy controller, since many trial errors can be encountered during its realisation and these controllers may not be suitable for other applications. The difficulties encountered in their design have guided researchers to move towards the optimisation of these controllers. This is why bio-inspired intelligence methods have been successfully applied to controller tuning in recent years[27].

The fuzzy MPPT controller receives the error and error variation of the rotational speed and the power of the turbine generator as inputs. It is based on the measurement of the wind power (ΔP_w) variation and the wind turbine speed ($\Delta\Omega$), to determine the variation ($\Delta\Omega_{\_ref}$) of the rotational speed setpoint ($\Omega_{\_ref}$), according to Eq. (19).

$$\begin{cases} \Delta P_w = P_w(k) - P_w(k-1) \\ \Delta\Omega = \Omega(k) - \Omega(k-1) \\ \Omega(k)_{ref} = \Omega(k-1) + \Delta\Omega(k)_{ref} \end{cases} \tag{19}$$

The wind turbine speed is controlled, in order to follow the reference speed ($\Omega_{\_ref}$), which is obtained at the output of the FLC. In addition, the output of the speed controller determines the reference of the electromagnetic torque of the studied machine (Fig. 5).

Figure 5 presents the triangular functions for the input variables of the FLC. For a high precision, the chosen FLC has seven linguistic variables, which can be defined as: Negative Big (*NB*), Negative Small (*NS*), Zero (*Z*), Positive Small (*PS*), and Positive Big (*PB*).

The quality of the input and output *FMs* can be expressed as follows[28,29]:

$-1 < P_1, P_8, P_{15} < -0.5$; $-0.5 < P_2, P_9, P_{16} < -0.3333$; $-0.3333 < P_3, P_{10}, P_{17} < -0.1667$; $-0.1667 < P_4, P_{11}, P_{18} < 0$; $0.166 < P_5, P_{12}, P_{19} < 0.3333$; $0.3333 < P_6, P_{13}, P_{20} < 0.5$; $0.5 < P_7, P_{14}, P_{21} < 1$.

The inference methods provide a resulting membership function $\mu(\Omega_{ref})$ for the output variable Ω_{ref}. It is, therefore, a question of fuzzy information and it must be transformed into determined information. The most widely used defuzzification method is that of determining the centre of gravity of the resulting membership function $\mu(\Omega_{ref})$.

The centre of gravity's abscissa is determined by[30]:

$$\Delta\Omega_{\_ref} = \frac{\sum_{i=1}^{M} \mu(\Delta\Omega_i).\Delta\Omega_i}{\sum_{i=1}^{M} \mu(\Delta\Omega_i)} \tag{20}$$

Metaheuristic optimisation techniques

The main inconveniences of the conventional optimisation technique P&O and fuzzy logic controllers are the gains estimation and robustness, especially for a nonlinear system such as a wind turbine or a permanent magnet synchronous generator (PMSG). Also, it becomes more difficult due to parameter uncertainties in the permanent magnet synchronous motor (PMSM).

Solving an optimisation problem involves finding the best solutions by maximising the objective function(s) of the problem, while satisfying a set of user-defined constraints. The best algorithms used to solve these

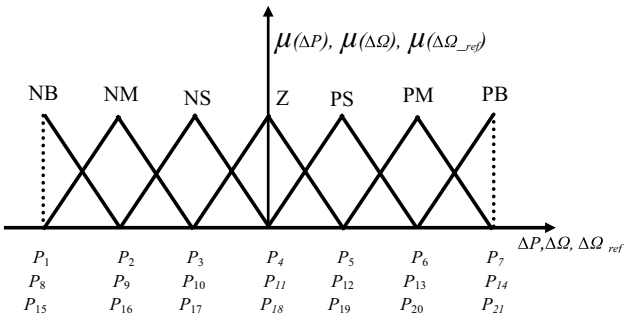

Figure 5. Membership functions of: ΔP_w, $\Delta\Omega$ and $\Delta\Omega_{\_ref.}$

optimisation problems are population metaheuristics. In order to provide a high performance and a high convergence speed in the system, two intelligent metaheuristic approaches (PSO and GA) are combined with the FLC.

The PSO algorithm

As the PSO algorithm is a metaheuristic optimisation approach, a number of particles can be dispersed in each search, which has very large spaces of candidate solutions. As each particle has a random speed, the algorithm depends on both the position and the speed of each particle.

Mathematically, the PSO algorithm uses a swarm made up of ($n_p \in N$) particles, i.e. $(\boldsymbol{X_i})_{i=1,2,\ldots.np}$, to search for the suboptimal X^*solution that minimises the objective function, called J. The velocity position of the particle vectors $\boldsymbol{i^{th}}$ are given by $\boldsymbol{X_i} = (\boldsymbol{X_{i,1}}, \boldsymbol{X_{i,2}}\boldsymbol{\ldots\ldots}\boldsymbol{X_{i,q}})$ and $\boldsymbol{V_i} = (\boldsymbol{V_{i,1}}, \boldsymbol{V_{i,2}}\boldsymbol{\ldots\ldots}\boldsymbol{V_{i,q}})$. They are determined by the following iterative expressions[31–34]:

$$\begin{cases} V_i^{l+1} = c_0.V_i^l + c_1.r_{1i}^l(X_i^{best,l} - X_i^l) + c_2 r_{2,i}^l(X_{swarm}^{best,l} - X_i^l) \\ X_i^{l+1} = X_i^l + V_{i,j}^{l+1} \end{cases} \tag{21}$$

where $l = 1,2,\ldots..l_{max}$ is the number of iterations previously provided by the user[8,9]. c_0, c_1 and c_2 are the inertia factor, the cognitive (individual) and social (group) learning relationships, respectively. $r_{1,i}^l$ and $r_{2,i}^l$ are random numbers which are evenly distributed over the interval [0,1], $X_i^{best,l}$ and $X_{swarm}^{best,l}$ are the best respective positions previously obtained by the particle and the best position obtained in the whole swarm at the current iteration l; they are given by:

$$\begin{cases} X_i^{best.l} = \min\left\{J(X_i^j), 0 \le j \le l\right\} \\ X_{swarm}^{best,l} = \min\left\{J(X_i^l), \forall i\right\} \end{cases} \tag{22}$$

Strategy of the genetic algorithm (GA)

The GA consists of the following steps[35,36]:

- *Step 1* Randomly generate N chromosomes in the initial population in the search space with the chromosome = $[\mathbf{X_1}, \mathbf{X_2}, \ldots, \mathbf{X_n}]$, where $X_{\min} \le X_{1,2,\ldots,n} \le X_{\max}$.
- *Step 2* Calculate the objective function for each chromosome.
- *Step 3* Apply the following operators:
  (a) Perform reproduction, i.e. pick the best probability chromosomes based on their objective function values.
  (b) Cross over the chromosomes selected in the above step using the crossing probabilities.
  (c) Perform a mutation on the chromosomes generated in the above step by probability of mutation.
- *Step 4* The process can be stopped if the stopping condition is reached or even the optimum solution is obtained. Alternatively, repeat steps 2 to 4 until the stop condition is met.
- *Step 5* The optimal solution X^*, corresponding to the best objective function $X^* = \min_{X_i^j}(J(X_i^j), \forall i, j)$ is thus obtained.

Fuzzy logic optimisation strategy using GA and PSO

According to the resolution of the optimisation problem, 21 fuzzy parameters can be determined. In addition, the objective function presents the sum of the Mean Square Error (MSE) values. Under a wind turbine value equal to 12.3 m/s, the error (which is the difference at each sampling time k) can be found between the optimum power supplied. Therefore the formula is obtained as follows:

$$J_k(k) = P_{opt}(k) - P_{sim}(k) \tag{23}$$

The objective function value (fitness function), during the search for the optimal solution, is presented in Fig. 6. The iteration number equals 70 when no reduction in total control error was detected.

The developed FL-GA controller is chosen for the final solution, trapped in a local optimal, which is considered to be a heuristic algorithm, where the best solution (Fig. 6a) is only recorded after several runs using several initialisations and settings of the GA parameters. Also, the choice of the GA to optimise the fuzzy logic control among those existing in the literature[9,24–27] is not unique. Therefore, the user is free to choose any other heuristic or metaheuristic optimisation algorithm, such as PSO; the best solution (Fig. 6b) is only recorded after several runs, using several initialisations and settings of the PSO. On the other hand, the optimisation of the parameters of fuzzy control must be performed using the same optimisation tool. This will ensure a fair comparison, in terms of control accuracy.

The tuning process of PSO/GA of the fuzzy MPPT controller, applied to the wind system, is shown in Fig. 7.

The fuzzy controller receives the error and the error variation of the wind generator power and the wind turbine speed as inputs. The turbine speed Ω is controlled so that it follows the reference speed (Ω_r_{ef}) obtained at the output of the fuzzy controller (FLC). In addition, the output of the speed controller determines the reference of the electromagnetic torque.

The developed controllers (LF-PSO and FL-GA) are defined to find the optimal values of the two controllers (fuzzy and PI). P_1, P_2, P_3, K_1, K_2, and K_3 are the normalisation factors of the FLC and k_{p2}, k_{i2} k_{p1}, and k_{i1} are the PI regulator gains, in order to minimise the given fitness function via Eq. (23).

Normalisation factors and error gains ensure the convergence response, stability and accuracy of the system. These factors affect the static error, damping and chatter, depending on the values of the gains before and after their optimisation.

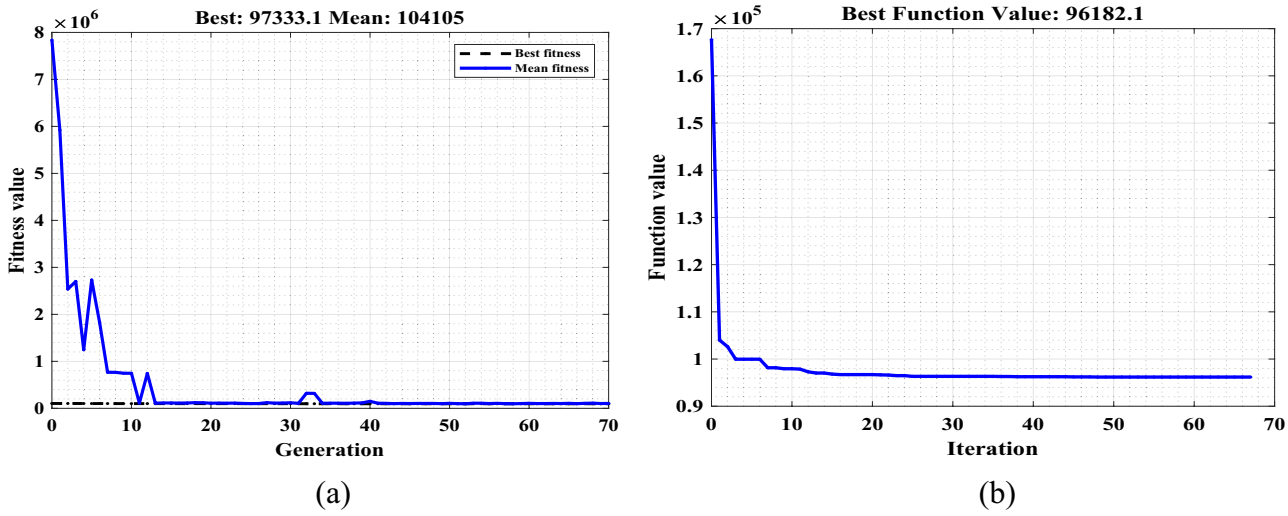

Figure 6. Objective function of (**a**): GA and (**b**): PSO.

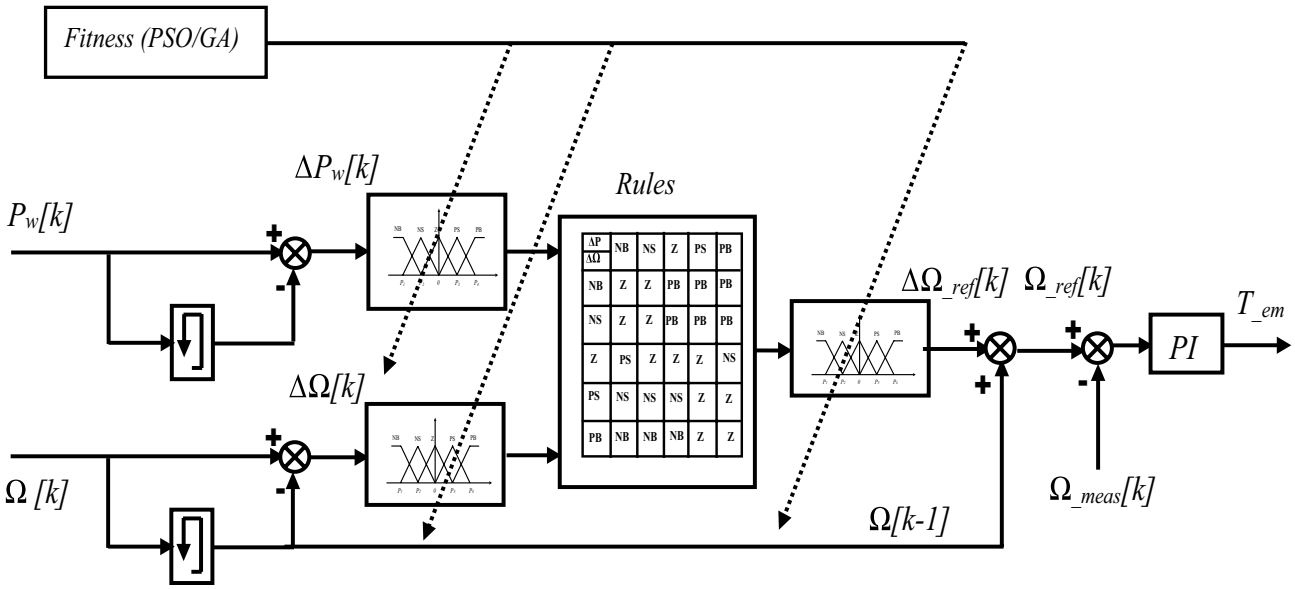

Figure 7. Schema of tuning process by PSO/GA of Fuzzy MPPT controller applied to the wind system.

Before optimisation, the membership function parameters of the inputs (ΔP, $\Delta\Omega$) and the output values ($\Delta\Omega_{ref}$) are obtained by manually varying the normalisation factors of the FLC and the gains of the PI regulator. Then, the optimisation by the developed controllers (LF-PSO, FL-GA), automatically sets the optimal values of the two controllers (FL and PI).

The membership function (MF) parameters, before and after the tuning process (PSO and GA), are presented in Tables 2, 3 and 4.

MF	P_1	P_2	P_3	P_4	P_5	P_6	P_7
Before PSO/GA	−1.000	−0.670	−0.340	0.000	0.3400	0.670	1.000
After PSO	−0.500	−0.373	−0.166	−0.125	0.0100	0.248	0.468
After GA	−0.518	−0.361	−0.315	−0.166	0.0373	0.212	0.423

Table 2. Membership function parameters of input (ΔP) before and after the PSO/GA.

MF	P_8	P_9	P_{10}	P_{11}	P_{12}	P_{13}	P_{14}
Before PSO/GA	− 1.000	0.670	− 0.340	0.0000	0.340	0.670	1.000
After PSO	− 0.704	− 0.493	− 0.166	0.0000	0.166	0.293	0.349
After GA	− 0.948	− 0.389	− 0.166	− 0.0001	0.154	0.300	0.450

Table 3. Membership function parameters of input ($\Delta\Omega$) before and after the PSO/GA.

MF	P_{15}	P_{16}	P_{17}	P_{18}	P_{19}	P_{20}	P_{21}
Before PSO/GA	− 1.000	− 0.670	− 0.340	0.0000	0.340	0.670	1.000
After PSO	− 0.978	− 0.334	− 0.329	− 0.0173	0.166	0.333	0.498
After GA	− 0.889	− 0.378	− 0.270	− 0.1160	0.135	0.333	0.486

Table 4. Membership function parameters of output ($\Delta\Omega_{ref}$) before and after the PSO/GA.

Simulation, discussion and results

A comparison of the results in recently published work (references[9,23–27]) was performed to show the validity of the proposed algorithm under fast changing conditions.

The simulation was carried out using Matlab/Simulink software. To test and compare the studied MPPT algorithms (P&O, FL and FL-PSO / GA), variable wind speeds were applied to the system and distributed over three intervals, as shown in Fig. 8. The algorithms were assessed in terms of speed, accuracy, and ripple.

- From 0.0 to 0.5 s, the wind speed is equal to 12 m/s.
- From 0.5 to 1.0 s, the wind speed is equal to 8 m/s.
- From 1.0 to 1.6 s, the wind speed is equal to 10 m/s.

Figures 9, 10, and 11 depict the MPPT controllers' dynamic and transient responses to variations in the turbine's optimal mechanical power, optimal speed and optimal torque. The analysed algorithms produced almost identical output curves.

By focusing on the transient state, the P&O, FL and FL-GA controllers provide an overshoot before convergence to the target, while the fuzzy-PSO controller converges directly and rapidly compared to the others.

The results reveal that the controllers are efficient and that all of the algorithms are suitable for the system during rapid changes in wind speed levels. The FL-PSO algorithm outperforms the other algorithms, in terms of reaction time, with a response time of nearly nil. The effect of optimisation is felt at low wind speeds.

For wind speeds of 12 m/s, 8 m/s, and 10 m/s, the values obtained at equilibrium are close to the ideal values for turbine speed and power, i.e. 74 rpm, 52 rpm, and 60 rpm and 5.5 kW, 1.5 kW, and 3 kW, respectively. The MPPT controllers lead the turbine to reach its maximum power point regardless of wind speed variation.

The output magnitudes of the PMSM are close to the optimal values regardless of wind speed variation, which demonstrates the robustness of the principle of the oriented rotor flux control (Figs. 12, 13 and 14).

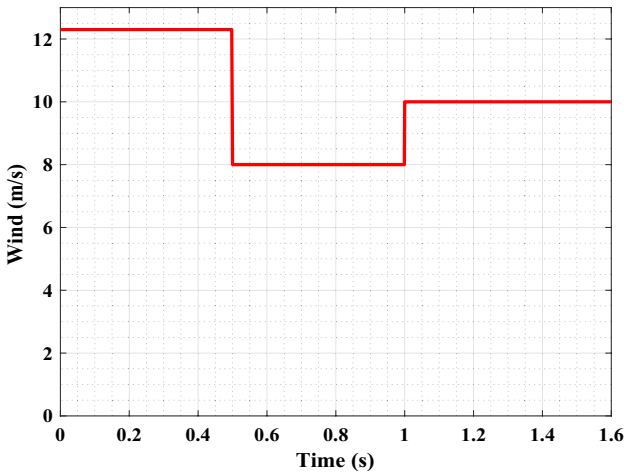

Figure 8. Variation in wind speed.

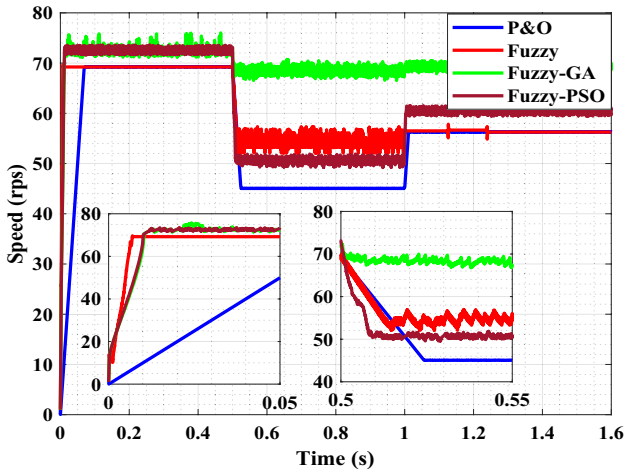

Figure 9. Optimal speed of the turbine.

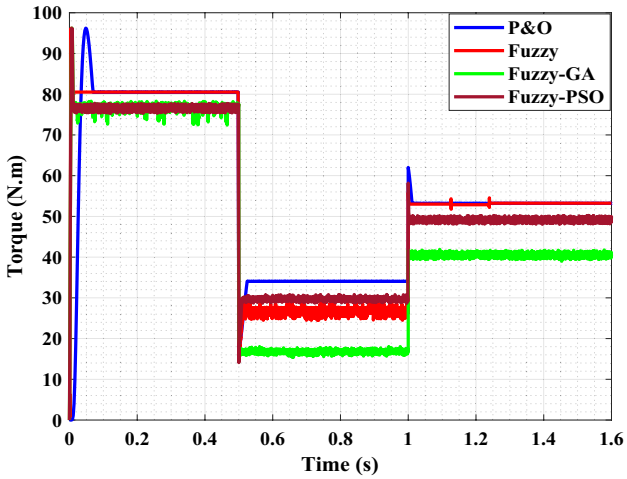

Figure 10. Optimal torque of the turbine.

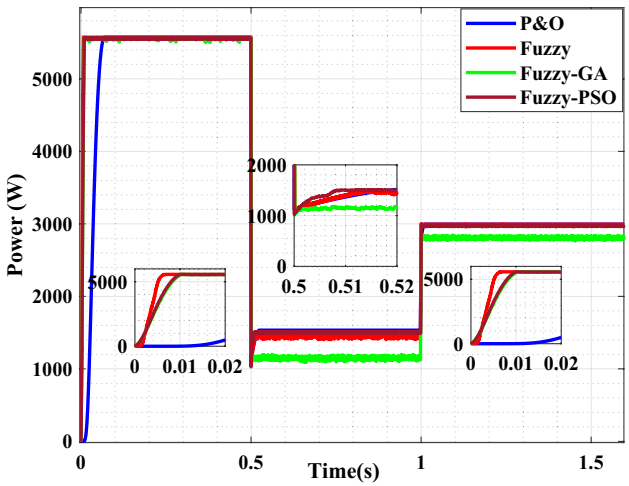

Figure 11. Optimal power of the turbine.

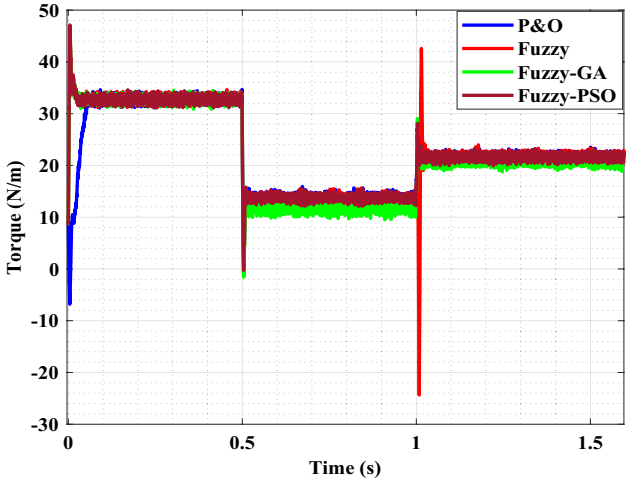

Figure 12. Optimal torque of the PMSM.

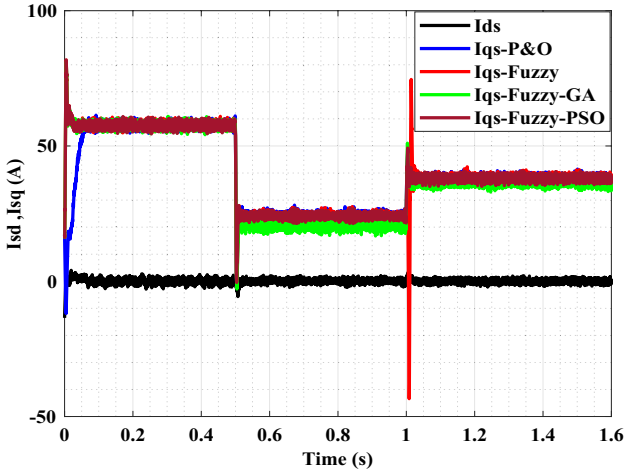

Figure 13. PMSM currents regulation.

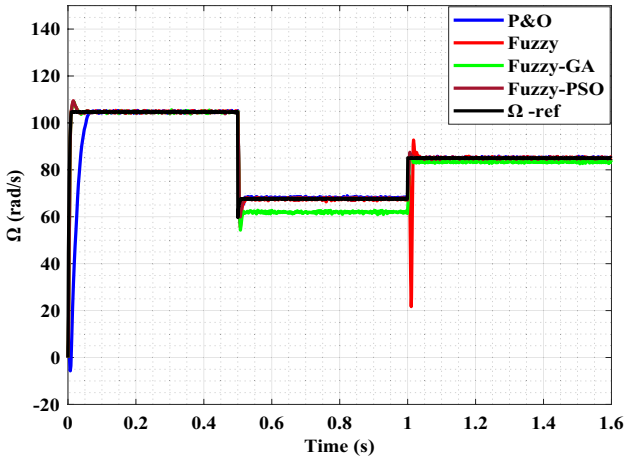

Figure 14. Regulation of th IM speed.

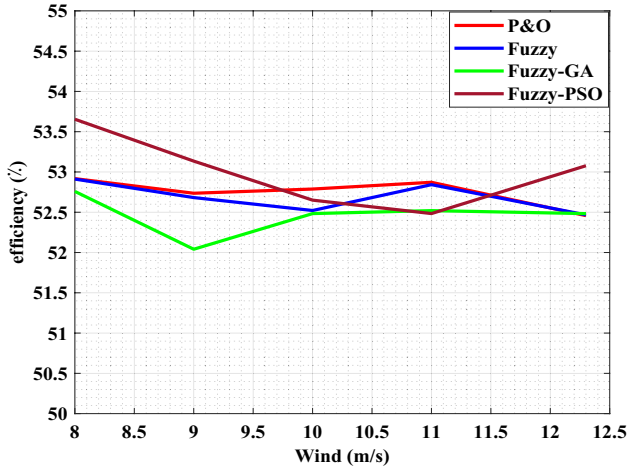

Figure 15. Efficiencies of the motor pump.

As illustrated in Fig. 12, the direct current component I_{ds} is adjusted to zero and the quadratic component I_{qs} is properly regulated in transient conditions. The perfect decoupling between rotor flux and torque is also clear, with the torque being the image of the quadratic current I_{qs} (vector control principle) (Fig. 13).

The speed tracking performance under wind constraints is very satisfactory (Fig. 14). The overall efficiency of the entire system (generator and motor pump) is approximately 50%. The efficiency of the motor pump for the different algorithms varies with the variation in wind speed. We notice that the efficiency of the Fuzzy-PSO algorithm is higher (53.6%) compared to the other algorithms (Fig. 15). The FL-PSO algorithm outperforms the other algorithms, in terms of reaction time (with a response time of nearly nil) and high efficiency.

To assess the robustness of the proposed algorithm in seeking the global MPP, the wind energy system has been subjected to non-uniform wind speeds from the start. It can be observed that the P&O and the FL methods had low complexity but present the lowest efficiency when compared to that of the developed FLC-GA and FL-PSO, which provided the highest efficiency.

The new combination between classical optimisation methods (P&O) and metaheuristic optimisation techniques performs better control, in terms of convergence time, and does not require knowledge about the wind turbine system.

Conclusion

This research presents a comparative study of the stability and overall efficiency of four MPPT controllers, applied to a wind turbine water pumping system driven by PMSM coupled to a centrifugal pump.

The results obtained showed that, whatever the variation in wind speed, the control system ran in a stable manner and always transferred all of the energy produced by the wind energy generator to the motor-pump unit.

The fuzzy logic controller optimised by PSO or GA eliminates the drawbacks of the conventional algorithm "P&O" and the fuzzy-PSO gives a high tracking performance compared to other controllers. Furthermore, the gains of fuzzy-PSO are self-tuned and can allow stability and robustness against parameter variations of the PMSM.

A comparative experimental study will be carried out to justify the performance of the MPPT algorithms presented in the paper, in addition the application of these methods in other systems such as WECS connected to the electricity grid, as well as isolated or autonomous systems containing storage batteries.

Data availability

The datasets used and/or analyzed during the current study are available from co-author Dr. Abdelaziz Rabehi (rab_ehi@hotmail.fr) on reasonable request.

Received: 2 April 2024; Accepted: 25 July 2024
Published online: 02 August 2024

References

1. Dykes, K. Dynamics of technology innovation and diffusion with emphasis on wind energy. Thesis: Ph. D. in Engineering Systems, Massachusetts Institute of Technology, Institute for Data, Systems, and Society. http://dspace.mit.edu/handle/1721.1/7582 (2016).
2. Davis, C. J. Computational modeling of wind turbine wake interactions. Master of Science Colorado State University (Fort Collins, Colorado, Spring, 2012).
3. Borni, A., Abdelkrim, T., Zaghba, L., Bouchakour, A., Lakhdari, A. & Zaarour, L. Fuzzy logic, PSO based fuzzy logic algorithm and current controls comparative for grid-connected hybrid system. In *AIP Conference Proceedings*, Vol. 1814 020006 (2017). https://doi.org/10.1063/1.497622
4. Mayouf, M. & Abdessemed, R. Comparative study of a small size wind generation system efficiency for battery charging. *Serb. J. Electr. Eng.* **10**(2), 261–274. https://doi.org/10.2298/SJEE120707003M (2013).
5. Bouchakour, A., Brahami, M. & Borni, A. Comparative study on photovoltaic pumping systems driven by different motors optimized with sliding mode control. *Int. J. Eng. Technol. Innov.* **7**(3), 201–216 (2017).

6. Esmaili, G. Application of advanced power electronics in renewable energy sources and hybrid generating systems. Doctoral Thesis, 2006, School of the Ohio State University. http://hdl.handle.net/10803/457978.
7. Sai Manoj, P., Vijayakumari, A. & Kottayil, S. K. Development of a comprehensive MPPT for grid-connected wind turbine driven PMSG. *Int. J. Energy Res.* https://doi.org/10.1002/we.2318 (2019).
8. Bouchakour, A., Borni, A. & Brahami, M. Comparative study of P&O-PI and fuzzy-PI MPPT controllers and their optimization using GA and PSO for photovoltaic water pumping systems. *Int. J. Ambient Energy* https://doi.org/10.1080/01430750.2019.1614988 (2019).
9. Ahmed, J. & Salam, Z. An improved perturb and observe (P&O) maximum power point tracking (MPPT) algorithm for higher efficiency. *Appl. Energy* **150**, 97–108. https://doi.org/10.1016/j.apenergy.2015.04.006 (2015).
10. Biricik, S. & Komurcugil, H. Proportional-integral and proportional-resonant based control strategy for PUC inverters. *IEEE* https://doi.org/10.1109/IECON.2018.8591371 (2018).
11. Phan, V. T., Lee, H. H. & Chun, T. W. An improved control strategy using a PI-resonant controller for an unbalanced stand-alone doubly-fed induction generator. *J. Power Electron.* https://doi.org/10.6113/JPE.2010.10.2.194 (2010).
12. Civelek, Z., Lüy, M., Çam, E. & Mamur, H. A new fuzzy logic proportional controller approach applied to individual pitch angle for wind turbine load mitigation. *Renew. Energy* https://doi.org/10.1016/j.renene.2017.04.064 (2017).
13. Abdelhalim, B., Abdelhak, B., Noureddine, B., Thameur, A. & Layachi, Z. Optimization of the fuzzy MPPT controller by GA for the single-phase grid-connected photovoltaic system controlled by sliding mode. In *AIP Conference Proceedings*, Vol. 2190 020003 (2019). https://doi.org/10.1063/1.5138489
14. Ed-dahmani, C. & Mahmoudi, H. A comparative study of fuzzy logic controllers for wind turbine based on PMSG. *Int. J. Renew. Energy Res.* **8**(3), 1386–1392 (2018).
15. Borni, A. *et al.* Comparative study of P&O and fuzzy MPPT controllers and their optimization using PSO and GA to improve wind energy system. *Eng. Model.* **34**(2), 55–76. https://doi.org/10.31534/engmod.2021.2.ri.05d (2021).
16. Bhattacharjee, C. & Roy, B. K. Advanced fuzzy power extraction control of wind energy conversion system for power quality improvement in a grid tied hybrid generation system. *IET Gener. Transm. Distrib.* **10**(5), 1179–1189. https://doi.org/10.1049/iet-gtd.2015.0769 (2016).
17. Yang, Y., He, Q., Fu, C., Liao, S. & Tan, P. Efficiency improvement of permanent magnet synchronous motor for electric vehicles. *Energy* https://doi.org/10.1016/j.energy.2020.118859 (2020).
18. Lin, C. H. & Lin, C. P. Voltage control of PM synchronous motor driven PM synchronous generator system using recurrent wavelet neural network controller. *J. Appl. Res. Technol. JART* **11**(2), 183–194. https://doi.org/10.1016/S1665-6423(13)71528-1 (2013).
19. Benbaha, N., Zidani, F. & Bouchakour, A. Seif Eddine Boukebbous: Optimal configuration investigation for photovoltaic water pumping system, case study: In a desert environment at Ghardaia, Algeria. *J. Eur. Syst. Autom.* **54**(4), 549–558. https://doi.org/10.18280/jesa.540404 (2021).
20. Štulrajter, M., Hrabovcova, V. & Franko, M. Permanent magnets synchronous motor control theory. *J. Electr. Eng.* **58**(2), 79–84 (2007).
21. Macana, C. A., Pota, H. R. & Hossain, M. A. Modeling and simulation of inverter based distributed generators for renewable energy integration. *IFAC PapersOnLine* **52**(4), 30–35. https://doi.org/10.1016/j.ifacol.2019.08.150 (2019).
22. Boukebbous, S. E. *et al.* Experimental performance assessment of photovoltaic water pumping system for agricultural irrigation in semi-arid environment of Sebseb: Ghardaia, Algeria. *Int. J. Energy Environ. Eng.* https://doi.org/10.1007/s40095-021-00435-8 (2021).
23. Bendibb, B., Belmili, H. & Krim, F. A survey of the most used MPPT methods: Conventional and advanced algorithms applied for photovoltaic systems. *Renew. Sustain. Energy Rev.* **45**, 637–648. https://doi.org/10.1016/j.rser.2015.02.009 (2015).
24. Ramli, M. A., Twaha, S., Ishaque, K. & Al-Turki, Y. A. A review on maximum power point tracking for photovoltaic systems with and without shading conditions. *Renew. Sustain. Energy Rev.* **67**, 144–159. https://doi.org/10.1016/j.rser.2016.09.013 (2017).
25. Youssef, A. R., Ali, A. I., Saeed, M. S. & Mohamed, E. E. Advanced multi-sector P&O maximum power point tracking technique for wind energy conversion system. *Electr. Power Energy Syst.* **107**, 89–97. https://doi.org/10.1016/j.ijepes.2018.10.034 (2019).
26. Bendaoud, M., Ladide, S., El Fathi, A., Hihi, H. & Faitah, K. Fuzzy logic peak current control strategy for extracting maximum power of small wind power generators. *Int. J. Energy Res.* https://doi.org/10.1002/etep.2730 (2018).
27. Assahout, S., Elaissaoui, H., El Ougli, A., Tidhaf, B. & Zrouri, H. A neural network and fuzzy logic based MPPT algorithm for photovoltaic pumping system. *Int. J. Power Electron. Drive Syst. (IJPEDS)* **9**(4), 1823–1833. https://doi.org/10.11591/ijpeds.v9.i4.pp1823-1833 (2018).
28. Ofosu, R. A., Odoi, B. & Asamoah, M. Electricity consumption forecast for Tarkwa using autoregressive integrated moving average and adaptive neuro fuzzy inference system. *Serb. J. Electr. Eng.* **18**(1), 75–94. https://doi.org/10.2298/SJEE2101075O (2021).
29. Miqoi, S., El Ougli, A. & Tidhaf, B. Adaptive fuzzy sliding mode based MPPT controller for a photovoltaic water pumping system. *Int. J. Power Electron. Drive Syst. (IJPEDS)* **10**(1), 414–422. https://doi.org/10.11591/ijpeds.v10.i1.pp414-422 (2019).
30. Attia, H. Fuzzy logic controller effectiveness evaluation through comparative memberships for photovoltaic maximum power point tracking function. *Int. J. Power Electron. Drive Syst. (IJPEDS)* **9**(3), 1147–1156. https://doi.org/10.11591/ijpeds.v9.i3.pp1147-1156 (2018).
31. Kennedy, J. & Eberhart, R. Particle swarm optimization. In *Proceedings of ICNN'95, International Conference on Neural Networks*. https://doi.org/10.1109/ICNN.1995.488968.
32. Farh, H. M., Eltamaly, A. M., Ibrahim, A. B., Othman, M. F. & Al-Saud, M. S. Dynamic global power extraction from partially shaded photovoltaic using deep recurrent neural network and improved PSO techniques. *Int. Trans. Electr. Energy Syst.* https://doi.org/10.1002/2050-7038.12061 (2019).
33. Harrag, A. & Messalti, S. PSO based SMC variable step size P&O MPPT controller for PV system sunder fast changing atmospheric conditions. *Int. J. Numer. Model.* https://doi.org/10.1002/jnm.2603 (2019).
34. Liu, B. *et al.* K-PSO: an improved PSO-based container scheduling algorithm for big data applications. *Int. J. Netw. Manag.* https://doi.org/10.1002/nem.2092 (2020).
35. Devasahayam, V. & Veluchamy, M. An enhanced ACO and PSO based fault identification and rectification approaches for FACTS devices. *Int. Trans. Electr. Energy Syst.* https://doi.org/10.1002/etep.2344 (2017).
36. Jumaa, N. K., Allawy, A. M. & Shubbar, M. S. Modelling and optimising a new hybrid ad-hoc network cooperation strategy performance using genetic algorithm. *Serb. J. Electr. Eng.* **18**(2), 193–210. https://doi.org/10.2298/SJEE2102193J (2021).

Acknowledgements

This publication was made possible by the support of the AUK Open Access Publishing Fund.

Author contributions

Conception: A.B., L.Z., N.B., M.B., A.B., L.Z., A.R., A.A., M.E.-A., S.S.M.G. Data collection: A.B., L.Z., N.B., M.B., A.B., L.Z., A.R. Formal analysis: A.B., L.Z., N.B., S.S.M.G. Methodology: M.B., A.B., L.Z., A.R., A.A., M.E.-A. Software: A.B., L.Z., L.Z., A.R., A.A. Supervision: L.Z., A.R., A.A., M.E.-A., S.S.M.G. Investigation: A.B., L.Z., A.R., A.A. Project administration: L.Z., A.R., A.A., M.E.-A., S.S.M.G. Funding acquisition: A.A.,

M.E.-A., S.S.M.G. Writing original article: A.B., L.Z., N.B., M.B., A.B., L.Z., A.R. Review the article: L.Z., A.R., A.A., M.E.-A., S.S.M.G.

Competing interests
The authors declare no competing interests.

Additional information
Correspondence and requests for materials should be addressed to M.E.-A.

Reprints and permissions information is available at www.nature.com/reprints.

Publisher's note Springer Nature remains neutral with regard to jurisdictional claims in published maps and institutional affiliations.